

Fluctuation Analysis of Short-Circuit Current in a Warm-Blooded Sodium-Retaining Epithelium: Site Current, Density, and Interaction with Triamterene

Ove Christensen and Niels Bindslev

Department of Medical Physiology A, University of Copenhagen, 3C Blegdamsvej, DK-2200 Copenhagen N, Denmark

Summary. Density and conductance of the Na-site in hen coprodeum were studied by employing fluctuation analysis of short-circuit current at sodium concentrations from 26 to 130 mM. Fluctuations of current in the frequency range 2–800 Hz were induced by triamterene, a reversible blocker of conducting epithelial Na-sites. At 130 mM Na the site density was $5.8 \pm 1.0 \mu\text{m}^{-2}$ and the site conductance was 4 pS. This conductance is equal to that of the frog skin (W. Van Driessche and B. Lindemann, 1979, *Nature (London)* **282**:519–520). Extrapolation of site density to zero sodium renders a total of 38 ± 28 sites μm^{-2} , which is compared with other estimates for the coprodeum. The site-triamterene association and dissociation constants were $9.5 \pm 0.4 \text{ rad sec}^{-1} \mu\text{m}^{-1}$ and $255 \pm 20 \text{ rad sec}^{-1}$ and they were independent of external sodium concentration. An analysis of the affinity constant for triamterene based on the DC-short-circuit current was found to be unrelated to the external sodium concentration and identical to that obtained from fluctuation analysis indicating a noncompetitive interaction between sodium and triamterene. Due to the oxygen demand of the epithelium we have developed an experimental method using short data processing times. A new analytical approach using integration of the power density spectrum proved necessary because of low signal-to-noise ratios.

Key words hen lower intestine · apical Na-site · current fluctuations · power density spectrum · triamterene · Na-site density

Introduction

The use of fluctuation analysis was introduced in biology in the mid-sixties (Verveen & Derksen, 1965). Current fluctuation analysis has recently been applied successfully to ion transport phenomena in tight epithelia (Lindemann & Van Driessche, 1977; Van Driessche & Zeiske, 1980; Lindemann, 1980) and leaky epithelia (Van Driessche & Gögelein, 1978).

The current fluctuation analysis exploits spontaneous conductance changes of random nature at equilibrium. The method is nonintrusive and allows one to obtain several basic transport characteristics of the epithelium such as the site density, the current through a single site and the rate constants for the association and dissociation between blocker and ion channel. In fact the site current and density may be obtained by the variance of short-circuit current (I_{sc}) and the I_{sc} .

Application of current fluctuation analysis in epitheliology is based on reversible blockers for conductive ion channels in epithelia. One clear example is the Na-channel in the apical membrane of sodium-retaining epithelia, such as the kidney cortical collecting duct, the colon, the urinary bladder, the frog skin and the cloaca, as presented here. This Na-channel is reversibly blocked by pyrazinoylguanidine analogs, e.g. amiloride and benzamil, and the pteridines such as triamterene (Cuthbert, Fanelli & Scriabine, 1979).

We have studied a Na-retaining epithelium from the midportion of the hen cloaca, the so-called coprodeum. The coprodeum is easily induced to absorb sodium by feeding the hens on a low sodium diet for more than 9 days (Choshniak, Munck & Skadhauge, 1977). The induced Na-transport seems to be due to an insertion of new integral protein molecules, 100 by 240 Å, in the luminal membrane of 20% of the coprodeal cells. Possibly these cells also acquire a dark, mitochondria-rich cytoplasm (Eldrup, Møllgård & Bindslev, 1979, 1980).

The present paper deals with the following questions.

The first point concerns the epithelium itself. Is the site density in agreement with the numbers obtained with independent methods and is the site current comparable to the current found in other epithelia? Site density obtained from the fluctuation analysis is contrasted with recent information on the number of induced sodium sites in the coprodeum and found to be about fivefold less than densities obtained from low-occupancy – displacement studies and morphological evidence. The site conductance is found to be in agreement with that in the frog skin (Van Driessche & Lindemann, 1979). This points to a common building-block in the evolution of the sodium-retaining mechanism.

The second question is how affinity constants determined from fluctuation analysis are related to

affinity constants obtained from concentration-response curves of the short-circuit current in steady-state experiments. It has been shown for coprodeum (Bindslev, 1979), that sodium in the mucosal medium in itself acts as a blocker on sodium sites. We find that the blocker triamterene reacts very fast with sodium sites compared to sodium. Due to the different magnitudes of relaxation times for triamterene and sodium, fluctuation analysis renders an affinity constant exclusively reflecting the site-triamterene interaction whereas the concentration-response of I_{sc} reflects the total reaction between site, triamterene and sodium.

The last question is a methodological one. Firstly, fluctuation measurements require the absence of signals which are inevitably induced by oxygenating the tissue. On the other hand oxygenation is necessary to maintain tissue function at 37 °C in warm-blooded animals. Secondly, sources of 'background' fluctuations exist which are not related to the action of triamterene on the mucosal membrane. These sources produce signals of the same magnitude as those induced by triamterene. In order to overcome these technical difficulties, we have used short measurement times (20 sec), during which the oxygen supply to the tissue is arrested. A new method for analyzing the power density spectrum of current fluctuations under these adverse conditions is presented. This method employs integration of the power density spectra for which reason we have named it the 'area'-method.

Materials and Methods

Materials

Hens, Diet, Tissue Handling and Transport Chambers. Egg-laying White Plymouth Rock hens weighing 3 to 4 kg were used throughout. The hens were given a low-sodium diet 2 to 4 weeks prior to experiment. The hens had free access to tap water. The diet results in an induction of a short-circuit current of about 200–300 $\mu\text{A cm}^{-2}$ in the coprodeum (Choshniak et al., 1977) due to an insertion of Na-sites in the luminal cell membrane (Bindslev, 1979). The coprodeum which is the mid-portion of the cloaca was isolated and stripped to the muscularis mucosae. Four to five pieces from the same coprodeum were mounted between perspex plates. The exposed area of tissue was 0.63 cm^2 . The mounted plates were inserted as mid-section of the transport chamber. One piece of tissue was studied at a time while the remaining were kept in oxygenated Ringer's at room temperature. The chamber was thermostatically heated to 34 °C. The half-chambers were constructed with large heat capacity so as to keep the temperature constant during data sampling where the heating was turned off. The half-chambers were open, thus allowing fast removal or fast addition of blocker solution. Oxygen was supplied and bathing solutions stirred by means of magnetic fleas in the bottom of the half-chambers in intervals between the data sampling periods. The construction of the chamber allowed a rapid interchange of plates mounted with tissue. The chamber was

placed on a 30-cm cushion of foam rubber, resting on top of a vibration-free table. The table was placed in a Faraday cage. All connections to the cage were interrupted during data sampling, except for the cables for voltage-clamping. The shields of these cables were connected to the cage.

Solutions, Sodium Channel Blockers and Electrodes. The basic Ringer's solution contained (in mM): NaCl 130, MgSO_4 0.5, CaCl_2 0.5, D-glucose 15, and was buffered with $\text{K}_2\text{HPO}_4/\text{KH}_2\text{PO}_4$ 2.5, pH 7.4, $\text{K}^+ = 4.5$. Lower Na concentrations were obtained by replacing NaCl with choline-Cl in equimolar amounts.

All studies of current fluctuations were made with the blocker triamterene, mol wt=253.26, which was kindly supplied by Mr. B. Faber, Ferrosan, Denmark. Triamterene was applied from a boiling Ringer's solution containing 1 mM triamterene by pre-cooling the pipette just before use. Triamterene is rather insoluble in aqueous media but we have found spectrophotometrically that the maximum triamterene concentration used at 37 °C (330 mM) stays dissolved for one-half hour. The pK_a for triamterene is 6.2 (Cuthbert, 1976). Thus at pH 7.4 only 6% of triamterene is in the protonated form. We have assumed that the protonated triamterene is the functional form of the blocker. Notice that all blocker concentrations are given as total concentrations. Amiloride-Cl dihydrate, mol wt=302.12 was obtained from Merck, Sharp & Dohme, Denmark. Amiloride was used in a concentration of 100 μM to obtain a complete blockage of sodium-carried current.

Ag/AgCl-electrodes were produced according to a recipe, mainly based on the work of Janz and Ives (1968). The interelectrode potentials were 0.1 mV or less. The resistance of an electrode pair amounted to about 1 k Ω for an electrode pair in Ringer's solution. Low-resistance voltage electrodes are necessary to avoid electrode noise on the input stage of the voltage amplifier.

The Electrical Set-up. The transepithelial voltage was clamped to 0 mV by a voltage clamp circuit. The voltage-sensing amplifier was designed around a matched pair of low-noise JFET-transistors as described by Van Driessche and Lindemann (1978). The noise of this amplifier, referred to the input stage, was 14 nV/(Hz)^{0.5} at 10 Hz. The AC-component of the short-circuit current above 0.02 Hz was amplified with a gain of 2×10^7 V/A. To prevent aliasing and perturbations from signals of low frequency the signal was passed through a band-pass filter (Krohn-Hite model 3750) with settings of 0.8 and 1.2 times the maximum and minimum analyzed frequencies. The roll-off at both frequencies was 24 dB per octave. The filtered signal of current fluctuations showed typical peak-to-peak amplitudes of 5 to 25 nA.

The whole voltage-clamp apparatus was powered from a battery box in order to avoid presence of any 50 Hz components in the signal.

Experimental Procedure

Measurement of Power Density Spectra. The filtered signal of current fluctuations was fed to a transient recorder (Gould Advance OS 4000 and output unit 4002) which samples and stores a record of 1024 data points. The data record was transferred digitally to a PDP-11/34 computer where the power density spectrum of the data record was calculated. This sequence was repeated a number of times and the power spectra of the individual data records were added to provide a mean power density spectrum. The resulting power spectrum consists of 512 data values (unit $\text{A}^2 \text{sec}$) which give the square of the amplitude of each of the frequency components in the signal. The final power spectrum

was stored for later analysis. The sequence of data acquisition, data transfer and computation of power spectrum was controlled by the computer.

The Actual Experiment. The power density spectrum of the short-circuit current fluctuations is affected by addition of a reversible blocker. The aim of the experiment is to find the relationship between blocker concentration and parameters characterizing the power density spectrum. The outcome of a typical experiment is ten power density spectra obtained at different blocker concentrations and a continuous record of the DC-short-circuit current. The first power density spectrum is measured at zero blocker concentration. The experiment is finished with application of 100 μM amiloride in order to get the level of short-circuit current due to pathways other than the blockable sodium sites. This spectrum represents a 'background' due to noise processes not associated with the action of the blocker.

Before measurement of power density spectra, the oxygenation, magnetic stirring and heating were switched off to avoid unwanted electrical signals in the AC-short-circuit current.

It is desirable to obtain as many data records as possible to get a well-determined power density spectrum. However, the time available for sampling current fluctuations is limited by the oxygen demand of the tissue. Actual practice is a trade-off between these two criteria and depends upon the frequency range suitable to study the particular blocker. The time required to Fourier transform a data record is around 1 sec. One data record is Fourier transformed while the following is sampled and hence the time consumed in processing one data record is 1 sec or the record sampling time, whichever is longer. Thus for triamterene the frequency range studied was 2–800 Hz and 20 records were taken to produce a power density spectrum.

Preliminary Experiments

Apical Driving Force. It has been shown for several Na-retaining epithelia that the intracellular potential becomes more depolarized when the electrodiffusional Na-influx is inhibited by blockers such as amiloride (Nagel, 1975; Frömter & Gebler, 1977; Helman & Fisher, 1977; Schultz, Frizzell & Nellans, 1977; Sudou & Hoshi, 1977). To obtain a measure of the intracellular potential upon addition of a blocker, triamterene, we measured the transmembrane resistance and short-circuit current.

The transmembrane resistance was measured by superimposing a small sinusoidal voltage (less than 1 mV) on the command voltage input of the voltage-clamping apparatus. This produces a small sinusoidal variation of the short-circuit current proportional to the transmembrane conductance. This variation was measured using a lock-in amplifier which is capable of detecting small signals that occur synchronously with the sinusoidal input. This method yields the true differential – or slope – resistance due to the small signal level.

The transmembrane resistance consists of the cell resistance in parallel with the intercellular shunt resistance. The latter was found as the value of resistance at 10^{-4} M amiloride. We assume that the cell resistance represents the Na-pathway in the luminal cell membrane. This is a somewhat gross approximation at the lowest blocker concentration, but probably correct within 30% since it is generally found that the serosal cell membrane make up 30% or less of the total cell resistance (Frömter & Gebler, 1977; Schultz et al., 1977). The potential across the luminal barrier is calculated as the product of the short-circuit current and the resistance of the Na-pathway measured at amiloride concentrations increasing from 0 to 10^{-4} M.

This procedure applied to 11 tissues rendered an initial cell potential (mean \pm SEM) of 68 ± 5 mV. The potential saturated with

increasing blocker concentration at a value of 111 ± 14 mV. At cell potentials of this size, the sodium current is approximately proportional to the cell potential which justifies the procedure used. The amiloride-blockable short-circuit current amounted to $177 \pm 8 \mu\text{A cm}^{-2}$. The shunt resistance was $290 \pm 18 \Omega \text{ cm}^2$ and the cell resistance at zero blocker concentration was $388 \pm 34 \Omega \text{ cm}^2$.

Derivation of the Fluctuation scheme

In this section we first introduce the assumed cell model. We then derive kinetic and fluctuation relations for a one-blocker and a two-blocker system. Thereafter we deal with theoretical implications of the derived relations.

Basic Model of Epithelial Cell

For the present application, the epithelial cell is conceived to operate according to the pioneering model of Koefoed-Johnsen and Ussing (1958): sodium enters through specific sites in the mucosal membrane down an electrochemical gradient and is pumped out of the cell at the basolateral membrane in exchange for potassium by the action of the Na/K-pump (ratio 3:2). Potassium which is pumped into the cell can leave by passive diffusion at the basolateral membrane. Voltage clamp to zero trans-epithelial voltage renders a large negative potential in the coprodeal cells (see preliminary experiments) and the cell Na-concentration is much smaller than that of the mucosal medium. Under these circumstances, the sodium influx across the luminal cell membrane is to a good approximation proportional to cell potential and to Na-concentration at the mucosal side.

Thus the relation between the sodium conductance g_{Na} , the short-circuit current I_{sc} and the cell potential V_c is approximately:

$$I_{\text{sc}} = g_{\text{Na}} V_c. \quad (1)$$

One-Blocker Kinetics

The action of diuretic drugs like triamterene or amiloride is to inhibit sodium transport by reversibly blocking the sodium entry sites in the mucosal membrane. The association and dissociation constants for this process are k_1 and k_2 . The blocker concentration is denoted B , the density of conducting (open) sites N_o and of blocked (closed) sites N_c . The corresponding kinetic scheme is



The total number of sites per unit area is N , which equals $N_o + N_c$. The rate equation correspond-

ing to this scheme is

$$dN_o/dt = -k_1 B N_o + k_2 N_c \quad (3)$$

for which the steady-state solution is

$$\begin{aligned} N_o &= P_o N = N/(1 + B/K_b) \\ N_c &= P_c N = N(B/K_b)/(1 + B/K_b). \end{aligned} \quad (4)$$

The affinity constant K_b is the ratio k_2/k_1 . P_o and P_c are the probabilities for a given site to be in the open or closed state.

The 'elementary' current through an open site is denoted i and hence the short-circuit current is given as

$$I_{sc} = N_o i \quad (5a)$$

which may be expressed as

$$I_{sc} = N i \frac{1}{1 + B/K_b}. \quad (5b)$$

Thus, from a plot of the reciprocal short-circuit current versus blocker concentration, i.e. a Dixon-plot, one can determine K_b as the x-axis intercept. As shown in the section 'Preliminary Experiments', cell potential, and accordingly i , increase and saturate with blocker concentration. This augmentation of current may result in an overestimate of K_b from Dixon-plots.

Two-Blocker Kinetics

It has been shown both for frog skin (Lindemann & Van Driessche, 1978) and for the hen coprodeum (Bindslev, 1979) that sodium in itself is a reversible blocker of the Na-entry site. Thus the Na-influx through the mucosal membrane of the coprodeum follows a Michaelis-Menten type relation with an affinity constant for sodium K_{Na} of about 5 mM.

Under the simultaneous action of triamterene and sodium blockers, Eq. (5) takes the general form (see also Segel, 1975):

$$I_{sc} = N i \frac{1}{1 + Na/K_{Na} + B/K_b + j(Na/K_{Na})(B/K_b)}. \quad (6)$$

Here, $j=0$ corresponds to competitive kinetics and $j=1$ corresponds to noncompetitive kinetics. In the latter case a state exists where both triamterene and Na are associated to the site although each one is sufficient to block the site.

At zero blocker concentration, the short-circuit current is given by

$$I_{sc} = N i \frac{1}{1 + Na/K_{Na}}. \quad (7)$$

The conclusion is that the short-circuit current saturates with the Na-concentration, since the site current i is nearly proportional to the Na-concentration at the mucosal side. Therefore, in order to estimate the total density N of Na-sites, measurements must be performed at several mucosal Na-concentrations. Furthermore, for the general case $0 \leq j \leq 1$, the apparent blocker affinity constant $K_{b'}$ is given by

$$K_{b'} = K_b \frac{1 + Na/K_{Na}}{1 + j Na/K_{Na}}. \quad (8)$$

$K_{b'}$ is independent of sodium concentration for non-competitive kinetics ($j=1$) and increases linearly with sodium concentration for competitive kinetics ($j=0$). For intermediate cases, $K_{b'}$ varies in a curvilinear fashion.

Properties of Current Fluctuations - One Blocker

When a reversible blocker is added to the mucosal membrane, an equilibrium situation arises in which the individual sodium channel participates in the process of association and dissociation with blocker molecules. The unblocked site associates with a blocker molecule within a characteristic time of $1/k_1 B$ and a blocked site stays blocked in a characteristic time of $1/k_2$ before dissociating the blocker. The total chemical rate constant for this process equals $k_1 B + k_2$ (Czerlinski, 1966; Lindemann & Van Driessche, 1977). The current through each site is switched on and off randomly. These events are assumed to be uncorrelated from site to site. The net result is that the short-circuit current fluctuates in time. The temporal and the amplitude characteristics of the fluctuating current may be used to infer the properties of the site-blocker kinetics and of the site current.

Current fluctuations are characterized experimentally by their power density spectrum (unit: $A^2 \text{ sec per cm}^2$ of tissue). At a given frequency f the power spectrum is $S(f)$. An overall measure of the fluctuating short-circuit current is the rms value of the signal, the square of which is the variance, $Var(I)$. The variance is related to the (two-sided) power density spectrum by the integral

$$Var(I) = 2 \int_0^\infty S(f) df. \quad (9)$$

(Although the lower limit of the integral formally is at zero frequency, the DC-component of the signal, I_{sc} , is not included since the variance refers to the AC-component of the short-circuit current only.)

From first principles, the variance of current

fluctuations is related to the microscopic site properties by the relation (Hill, 1971)

$$\text{Var}(I) = Ni^2 P_o P_c. \quad (10a)$$

Inserting Eqs. (4) and (5) in Eq. (10a), this may be written as

$$\text{Var}(I) = I_{sc} i (B/K_b) / (1 + B/K_b). \quad (10b)$$

Thus simultaneous measurements of $\text{Var}(I)$ and I_{sc} at different blocker concentrations make it possible to determine the site current and, through Eq. (5b), the density of Na-sites. This determination is independent of the particular blocker used since N and i are properties of the tissue, not of the blocker.

The characteristics of the site-blocker reactions are brought about in the Lorentzian form of the power spectrum characteristic for one-blocker kinetics (Verveen & DeFelice, 1974)

$$S(f) = S_o / (1 + (f/f_c)^2). \quad (11)$$

$S(f)$ is characterized by the plateau value S_o and the corner frequency f_c . The corner frequency is related to the association and dissociation rate constants by the relation (Verveen & DeFelice, 1974)

$$2\pi f_c = k_1 B + k_2. \quad (12)$$

Measurement of corner frequencies at various blocker concentrations thus serves to determine the kinetic constants of the site-blocker interaction. The relation between the plateau value S_o , the corner frequency f_c and the variance is, by combining Eqs. (9) and (11),

$$\text{Var}(I) = \pi f_c S_o. \quad (13)$$

Properties of Current Fluctuations - Two Blockers

In general, the power spectrum of current fluctuations due to the action of two blockers may be found from the kinetic reaction scheme by using the matrix method of Chen (1975). However, this knowledge is not straightforward to use in order to determine the kinetic constants of the two blockers from measured power density spectra.

For the blockers triamterene and sodium, it is possible to simplify matters greatly by using some simple experimental facts for the action of these blockers on the hen coprodeum. Thus the typical corner frequencies for triamterene are from 50 to 200 Hz corresponding to reaction times site-triamterene in the millisecond range. On the other hand the influence of sodium in the power spectrum was found to be important only below 1 Hz. The fre-

quency range employed in the present studies with triamterene is from about 2 to 800 Hz. Consequently the site-sodium kinetics does not manifest itself in the experimental power spectra.

We shall hence assume that the power spectrum consists of essentially a single Lorentzian with a corner frequency reflecting the total chemical rate of the site-triamterene kinetics according to Eq. (12). For the analysis of the short-circuit current the two-blocker situation is not the same as the simple one-blocker case because this current reflects blocking of sites both by triamterene and by sodium.

It turns out, however, that the results for properties of current fluctuations obtained in the one-blocker case are still correct for two blockers in the formulation summarized below:

$$I_{sc} = \frac{Ni}{1 + \text{Na}/K_{Na}} \frac{1}{1 + B/K_b}, \quad (6)$$

$$K_{b'} = K_b \frac{1 + \text{Na}/K_{Na}}{1 + j \text{Na}/K_{Na}}, \quad (8)$$

$$\text{Var}(I) = I_{sc} i (B/K_b) / (1 + B/K_b), \quad (10b)$$

$$2\pi f_c = k_2 (1 + B/K_b), \quad (12)$$

$$S_o = \frac{2I_{sc} i}{k_2} \frac{B/K_b}{(1 + B/K_b)^2}. \quad (14)$$

The crucial point in the formulation of these equations is that the influence of sodium on the variance in Eq. (10b) is expressed through the short-circuit current. One may say that the slow interaction between sodium and site is accounted for in this way. The form of the power spectrum given by Eqs. (11), (12) and (14) is identical to the one derived by Lindemann and Van Driessche [1978, Eqs. (13) and (14)] for the case of competitive kinetics and it can be shown that this result is valid in the general case $0 \leq j \leq 1$. The condition for this is, as mentioned above, that the time constants for site-sodium interactions are much larger than for the site-triamterene interaction.

Discussion of Theoretical Results

Analysis of the short-circuit current [Eq. (6)] yields an apparent affinity constant $K_{b'}$ for blockers in the two-blocker case. A study of $K_{b'}$ for triamterene versus Na-concentration serves to determine the degree of competition between sodium and triamterene according to Eq. (8). Contrary to this the variation of corner frequency with triamterene concentration [Eq. (12)] yields the true value of the affinity constant K_b , i.e. a value which is not obscured by the influence of the slow site-sodium kinetics.

The site current i may be obtained from Eq. (10b). A plot of $\text{Var}(I)/I_{sc}$ versus blocker concentration gives a Michaelis-Menten type curve with a saturation value equal to the site current and an affinity constant of K_b . At zero blocker concentration, the short-circuit current is given by Eq. (7). With the value determined for i , one can hence obtain the apparent site density N' at a given sodium concentration:

$$N' = \frac{N}{1 + Na/K_{Na}} \quad (7a)$$

S_o is in practice determined from $\text{Var}(I)$ and f_c through Eq. (13). Therefore, it does not supply more information than already obtained.

The analysis of the variation of corner frequency with blocker concentration is the most direct assessment of the kinetic parameters because it does not depend on the site current and hence is correct regardless of variations in cell potential caused by the change of mucosal sodium permeability with application of a blocker.

It follows from Eqs. (6) that the short-circuit current decreases in a hyperbolic fashion with blocker concentration. The fluctuations in the short-circuit current, expressed by the variance of Eq. (10b) vanish both at zero blocker concentration and at very large blocker concentration and have maximum values in between. For a one-blocker system, this maximum occurs at a blocker concentration of K_b .

Data Analysis

In this section we first describe a conventional method to obtain parameters from power density spectra and second we derive a new method for analyzing these spectra, because this new method proved to be decisive for the signal analysis due to low signal-to-noise ratio in the coprodeum. The new method is superior to the conventional and allows one to use fewer data records still with better resolution. We call this new method the 'area method'. The site density and the site current are found from simultaneous measurements of variance and the I_{sc} . Finally the extraction of k_1 and k_2 from the data is dealt with.

Analysis of Power Density Spectra

In Fig. 1 is shown power density spectra obtained from the hen coprodeum at 34°C. The lowermost spectrum is the background spectrum obtained at the end of the experiment by addition of 100 μM amiloride and therefore represents current fluc-

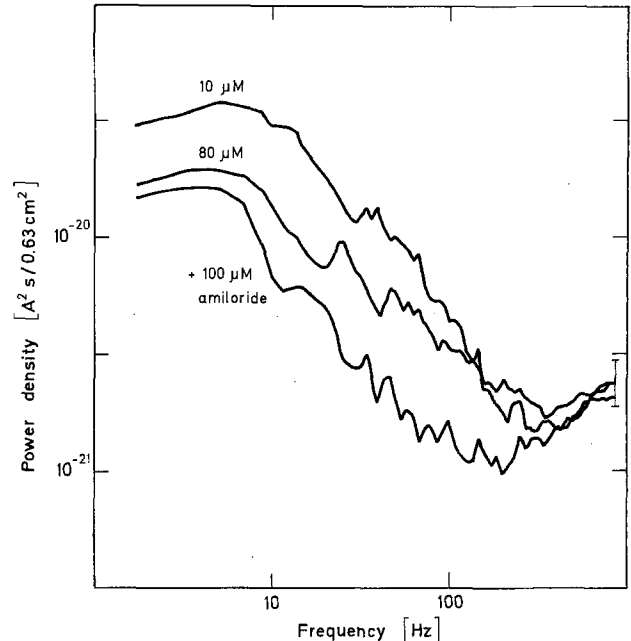


Fig. 1. Power density spectra for triamterene-induced fluctuations in short-circuit current through the coprodeum when clamped to zero transepithelial voltage at 34°C. The two upper spectra are obtained at triamterene concentrations of 10 and 80 μM in the mucosal solution. The lowermost spectrum is the background spectrum obtained by further addition of 100 μM amiloride to the mucosal solution. The spectra are measured at a sodium concentration of 26 mM in the bathing solutions. Each spectrum is based on 20 data records. The bar indicates the typical scatter of data points at high frequencies. The slight roll-off towards lower frequencies is due to the high-pass filter cut-off at 2 Hz.

tuations not related to site-triamterene interactions at the mucosal membrane. Additional noise is introduced when various concentrations of triamterene, 10 and 80 μM in the Figure, are added to the mucosal solution (before final addition of amiloride). The spectra at zero blocker concentration and at 100 μM amiloride are to a good approximation identical and hence the background is practically independent of mucosal triamterene concentration. It follows that the additional noise is due to the action of triamterene at the mucosal membrane. It is seen from the Figure, that the triamterene-induced noise shifts toward higher frequencies with increasing triamterene concentration. On the other hand, the triamterene-induced noise is not sufficiently large to allow a direct identification of corner frequency f_c and plateau value S_o of the Lorentzian spectrum Eq. (11). Fishman (1973) has solved a similar situation for K-channel noise in the squid axon membrane by subtracting a background spectrum. In the present case, the background spectrum is obtained after final addition of 100 μM amiloride. This may be subtracted from the spectra obtained with triamterene.

Although such a procedure is possible in principle, it has serious drawbacks. Notice in Fig. 1 that the value of the power density spectrum at given frequency is associated with a rather large variation of statistical nature. Thus a difference spectrum will be determined as the small difference between two large quantities. Typically for the hen coprodeum, the maximum variance is only 130 to 200% of the variance associated with the background spectrum! The statistical error connected with the difference will thus at most frequencies exceed the difference spectrum. The statistical error may, in principle, be brought down to a manageable level by increasing the number of data records used to construct a single spectrum. This solution is not possible for the hen coprodeum since the tissue has a high oxygen demand and oxygenation must be turned off during data sampling of current fluctuations.

The 'Area' Method for Analyzing Power Density Spectra

In view of these difficulties, we have devised a new and very powerful method of analyzing power density spectra.

In the following, let us denote by S_b the background power density spectrum and by S_{ib} the spectrum due to combined background and triamterene-induced current fluctuations. The analysis presumes that the difference $S_{ib} - S_b$ has a Lorentzian shape [Eq. (11)] and the question is to determine the characteristic parameters f_c and S_o .

To do this, we evaluate the accumulated area $A(f)$ under the power density spectrum up to a given frequency f :

$$A(f) = 2 \int_0^f S_{ib}(f) df - 2 \int_0^f S_b(f) df. \quad (15)$$

For a Lorentzian spectrum, integration of Eq. (11) yields

$$A(f) = 2 \int_0^f \frac{S_o}{1 + (f/f_c)^2} df = 2S_o f_c \arctg(f/f_c). \quad (16)$$

Integration of the power density spectrum is a very efficient way to eliminate the influence of statistical variations in the difference spectrum. Thus instead of fitting the difference spectrum directly to a Lorentzian, we fit the integrated difference spectrum to an arctg-curve according to Eq. (16).

In Fig. 2 is shown a plot of $A(f)$ versus frequency and also a plot of the theoretical best fit arctg-curve. The parameters S_o and f_c can be determined from the experimentally obtained accumulated area $A(f)$. The saturation value of the accumu-

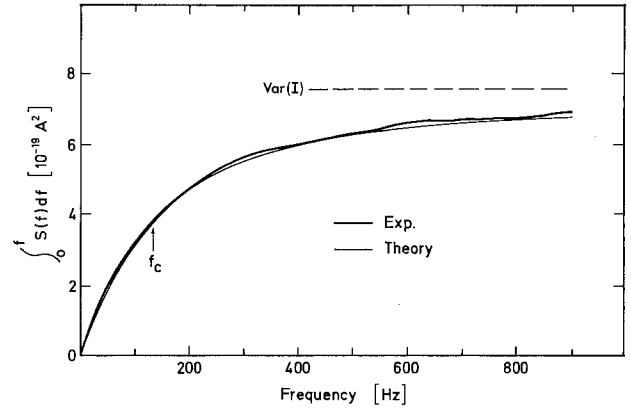


Fig. 2. Integral of differential power density spectrum up to a given frequency as a function of this frequency. (The integral of power density over a frequency interval equals the contribution to the variance of current fluctuations in this frequency interval.) The experimental curve (heavy line) is determined for a triamterene concentration of $80 \mu\text{M}$ at 26 mM sodium in the mucosal bathing solutions. The theoretical curve (thin line) is the arctg-curve from Eq. (16) based on integration of a Lorentzian power density spectrum. This curve is characterized by the corner frequency f_c and the variance, $\text{Var}(I)$, shown in the Figure

lated power density area equals by definition the variance, $\text{Var}(I)$. Now since

$$A(f_c) = S_o f_c \pi/2 = 1/2 \text{Var}(I) \quad (17)$$

one finds f_c as the frequency where the accumulated area assumes one half of the saturation value. S_o is found from Eq. (13). Figure 2 illustrates a case where $\text{Var}(I)$ is not reached within the experimentally employed frequency range. In this case we consider the obtained value of f_c as a first-order approximation. If the maximum frequency employed experimentally is f_{max} the second order approximation to $\text{Var}(I)$ can be found from

$$A(f_{\text{max}}) = \text{Var}(I) 2/\pi \arctg(f_{\text{max}}/f_c)$$

by inserting into this the first-order approximation to f_c . From this value of the variance one can next obtain the second-order approximation to f_c . Usually first- and second-order approximations did not for the present experimental material deviate more than maximally 30% and further iterations were not necessary.

The area method above is very well-suited to automatic numerical computation of $\text{Var}(I)$, f_c and S_o . This is of great practical importance since, for the present data material, about 3–400 spectra were analyzed. Based upon regression analysis between the experimentally determined accumulated area $A(f)$ and the theoretical arctg-curve, rational criteria were used in the evaluation of the goodness of fit and boarderline cases were examined on a graphical display screen.

At frequencies above 300 Hz, the spectra (Fig. 1) are dominated by amplifier noise which varies with the impedance of the tissue. This contribution to the background noise varies with blocker concentration. With the values given for cell and shunt resistance in 'preliminary experiments' it follows that at rea-

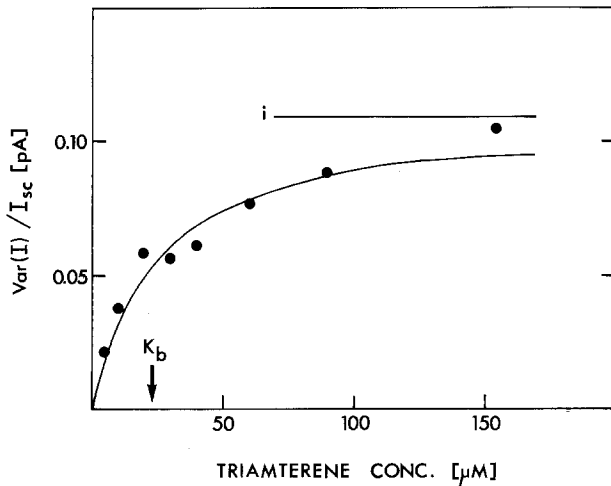


Fig. 3. Analysis of variance of current fluctuations. The ordinate is $\text{Var}(I)/I_{sc}$ which has a Michaelis-Menten type dependence upon the blocker concentration (full curve) with a saturation value to the site current i [cf. Eq. (10b)]. The sodium concentration is 52 mM

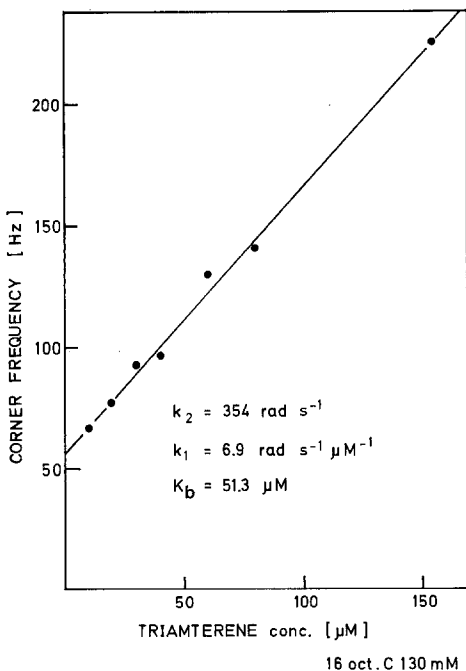


Fig. 4. Corner frequency, as determined by the area method, as function of the mucosal triamterene concentration at 130 mM sodium concentration. Except for a factor of 2π , the dissociation constant k_2 is found as the y-axis intercept of the straight line relationship. The association constant k_1 is the slope of this line. The affinity constant, K_b , for the site-triamterene interaction is found as the x-axis intercept of the line

sonably high blocker concentrations, the tissue impedance is to an excellent approximation constant and hence amplifier noise cancels in the difference spectra. At small blocker concentrations, this is not quite obtained but the corner frequencies here are small and amplifier noise is not important in the region of the spectra which determines f_c .

One should not forget that although the difference between a spectrum and the background spectrum is small at high frequencies, the high-frequency region contains much information due to the large amount of data present here. Fig. 2 clearly shows that the integrated difference spectrum increases at high frequencies such that the information here is effectively employed by the area method. Contrary, a Lorentzian fit to the difference spectrum would be restricted to frequencies below about 100 Hz (cf. Fig. 1).

The procedure outlined above was successful in most cases. The only exceptions were cases in which the background spectrum varied with increasing blocker concentration, i.e. the variance of current fluctuations was significantly different at zero blocker concentration and at 100 μM amiloride. Such cases were discarded. Another exception were some preliminary studies with the blocker benzamil, for which the corner frequencies were so low that interaction with sodium showed up in the spectra. The main reason for choosing triamterene as a blocker in the present experiments was the wide separation of corner frequencies for triamterene and sodium.

Determination of Site Density from Variance

In order to determine the apparent site density and the elementary current through the single Na-site, we proceed from Eq. (10b). Figure 3 shows a plot of the experimentally determined quantity $\text{Var}(I)/I_{sc}$ versus triamterene concentration. It is seen that the data points follow approximately the theoretical Michaelis-Menten type of relation with a saturation value which, according to Eq. (10b), equals the site current i . The apparent site density [Eq. (7a)] is then determined from the short-circuit current at zero triamterene concentration.

The site current and density are derived from the variance of current fluctuations which in the present work is found from numerical integration of the power density spectrum and thus involves a fair amount of computational work. But the variance may, in principle, be determined from analog measurements of the rms-value of the fluctuating current and therefore does not require the same degree of sophistication as when a computer is employed in the experiments.

Notice that the site density is a membrane-specific parameter whereas the site current is influenced by the value of the cell potential and mucosal sodium concentration.

Determination of Rate Constants k_1 and k_2

In Fig. 4 is shown a plot of corner frequency versus triamterene concentration. The data follow the straight-line relationship predicted from Eq. (12). The x-axis intercept gives the affinity constant K_b characteristic for the site-triamterene interaction. The rate constants k_1 and k_2 are, except for a factor of 2π , determined as the slope of the line and the y-axis intercept.

The triamterene concentrations used in this study were 5, 10, 20, 30, 40, 60, 80, 154 and 290 μM . The range of concentrations which permitted analysis of corner frequencies were usually in the range of about 10 to 80 or 154 μM since the blocker-induced current noise is small at concentrations much smaller than or much larger than K_b [cf. Eq. (10b)].

Results and Discussion

The following results are derived on the assumption that the current through the Na-site is independent of the blocker concentration. The blocker is thought only to close and open Na-sites as it jumps on and off the site.

Site Current and Site Density in Coprodeum

Figure 5 shows the variation of the current through a single Na-site as well as the variation of the site density with the Na-concentration. Site density here means the number of sites per μm^2 that can be blocked by triamterene. The site current i increases approximately linearly with the Na-concentration. In the section on Preliminary Experiments it was shown that with increasing concentration of blocker, the cell potential drops from about -70 mV to saturation at about -110 mV. The value of i determined from analysis of variance thus corresponds to a potential between these. At 26 mM Na there is a tendency for the site current to be somewhat higher than expected in case the site current was proportional to the Na-concentration. A pure Na-current through the site extrapolates to zero with no Na in the bathing media.

A linear relationship of site current and Na-concentration was found for the frog skin (Van Driessche & Lindemann, 1979). The current through the site in the coprodeum is comparable to that of the frog skin. At 130 mM Na the site-conductance is

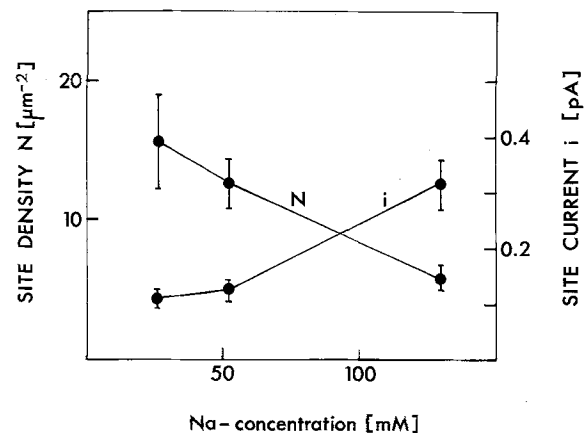


Fig. 5. Experimentally determined density of Na-sites on the mucosal membrane N and the current through a single site i as function of sodium concentration in the external solutions. The curves show mean and SEM based on 7 to 16 observations at each concentration

4 pS in the coprodeum based on an estimated intracellular potential of -80 mV. The corresponding value in the frog skin is 5.5 pS at 110 mM Na. The agreement between the two conductances seems to indicate that the fundamental processes for the transfer of sodium ions are the same in these two epithelia.

The site density increases as the Na-concentration is reduced. A reduction of the Na-concentration from 130 to 26 mM increases the site density by a factor of 2.7. The site density is assumed to follow the Na-concentration in a hyperbolic fashion, as given by Eq. (7a). A nonlinear least-squares fit to the data points yields a K_{Na} of 32 ± 22 mM Na and a maximal site density of $38 \pm 28 \mu\text{m}^{-2}$. The large standard deviations on the data points are primarily due to huge interanimal variations. This is therefore a rather inaccurate determination of K_{Na} and of the density at zero Na-concentration, but experiments at Na-concentrations lower than 26 mM could not be resolved due to a small signal level at the lower Na-concentrations.

The short-circuit current, equal to $N_0 i$, follows an MM-type kinetic as determined by transmural flux measurements (Lyngdorf-Henriksen, Munck & Skadhauge, 1979) and by influx of Na across the luminal cell membrane in coprodeum (Bindsløv, 1979) with a K_{Na} of 6 and 5 mM Na. Thus there seems to be a discrepancy between the K_{Na} determined from flux measurements and the present one, but in recognition of the large standard deviation on K_{Na} it is premature to go into a discussion of this discrepancy.

The density of sodium sites in the coprodeum has been evaluated by two other methods. The num-

bers of specific binding sites per μm^2 has been determined for ^3H -benzamil at low occupancy, 1 nM, in the absence of Na. This resulted in seven specific binding sites for benzamil in the coprodeum from hens on a low Na diet, whereas there were no such sites in coprodeum from hens on a high Na diet (Cuthbert, Bindslev, Skadhauge & Edwardson, *in preparation*).

A rough estimate of the site density at full occupancy may be obtained by extrapolation. The site density comes out to be between 175 and $350 \mu\text{m}^{-2}$ at zero Na. This value may be compared with the density obtained from fluctuation-analysis of $38 \pm 28 \mu\text{m}^{-2}$.

Studies comparable to these have been carried out on frog skin. From binding-displacement studies with amiloride and benzamil Cuthbert (1973) and Acheves, Cuthbert and Edwardson (1979) obtained 400 and $130 \mu\text{m}^{-2}$ and VanDriessche and Lindemann (1979) measured around 15 sites μm^{-2} by fluctuation-analysis using amiloride, all at zero Na-concentration. The densities of Na-sites in the coprodeum are thus of the same order of magnitude as in the frog skin.

For the coprodeum a third estimate for the numbers of Na-sites may be obtained based on morphological studies. In freeze-fracture there appear new characteristic intramembraneous particles with a rod-shaped form, 100 by 240 \AA , in the luminal cell membrane of the coprodeum when birds are given a low Na diet. These rod-shaped particles span the apolar domain of the plasma membrane and may well be the Na-channel (Eldrup et al., 1979, 1980). Although these authors did not state a number for the density of rod-shaped particles, we have made an order-of-magnitude estimate of the particle density to about $300 \mu\text{m}^{-2}$.

The simplest explanation for the different densities of the three estimates of Na-sites in the coprodeum is that a great deal of the inserted rod-shaped particles in the luminal cell membrane are inactive even when the concentration of Na is lowered toward zero and that benzamil also binds to some or most of these inactive sites.

Triamterene Rate Constants as Functions of Na-Concentration

The association and dissociation rate constants for the interaction between site and triamterene, k_1 and k_2 , are shown in Fig. 6 as function of the Na-concentration in the bathing solutions.

Both rate constants are nearly independent of the Na-concentration. This was expected since the two rate constants are considered as representing exclusively the interaction between the site that sees

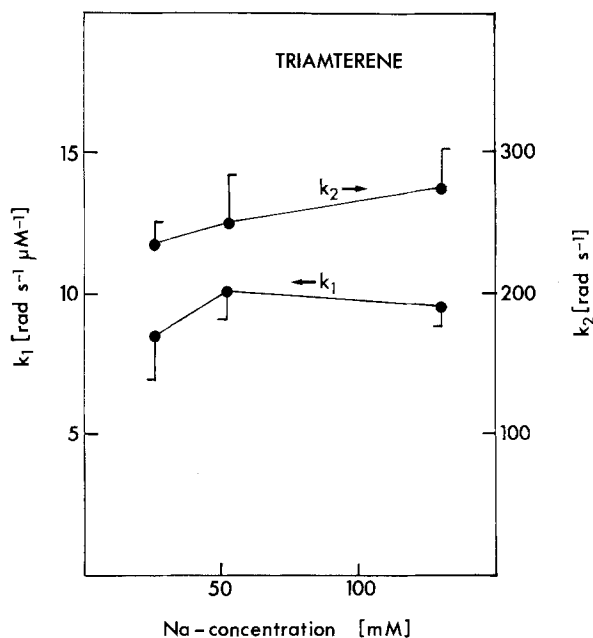


Fig. 6. Variation with sodium concentration of association rate constant k_1 and dissociation rate constant k_2 for the site-triamterene interaction at 34°C . Data are mean and SEM based on 7 to 8 observations

triamterene and the triamterene molecule, such that k_1 and k_2 for this reversible reaction are not modified by sodium. Constant fit to k_1 and k_2 gives $k_1 = 9.5 \pm 0.4 \text{ rad sec}^{-1} \mu\text{M}^{-1}$ and $k_2 = 255 \pm 20 \text{ rad sec}^{-1}$.

Only in cases where two blockers have rate constants of comparable magnitude will changes in the concentration of one blocker interfere with the determination of the rate constants for the other blocker. Such an interference was discovered for Na and benzamil in the coprodeum. The two blockers both have corner frequencies in the 1-Hz range (Christensen & Bindslev, *unpublished*).

In the coprodeum k_1 for triamterene is independent of changes in the Na-concentration. The same independence of the Na-concentration of k_1 was found in the frog skin for amiloride (VanDriessche & Lindemann, 1979). The weak dependence of k_2 for triamterene in the coprodeum on changes in Na-concentration could be due to a change in the surface properties as the sodium ion is replaced by choline ions. In contrast to this a rather steep dependence was found in the frog skin for k_2 for amiloride on the Na-concentration. However, this determination was rather uncertain (VanDriessche & Lindemann, 1979).

In this connection where the purpose is to determine 'pure' transport parameters it may be stressed that the fluctuation analysis also elegantly circumvents the problems related to unstirred water layers.

K_b as a Function of the Na-Concentration

The ratio k_2/k_1 gives K_b based on current fluctuation-analysis, $K_b(f_c)$, which is the true affinity constant for triamterene. The $K_b(f_c)$ is shown in Fig. 7 as a function of the Na-concentration and found to be essentially independent of the Na-concentration, $K_b(f_c) = 30.8 \pm 2.4 \mu\text{M}$.

In Fig. 7 is also shown $K_{b'}$ determined from Eq. (5) in plots of $1/I_{sc}$ against the blocker concentration. This affinity constant is denoted $K_{b'}(I)$. The potential across the luminal cell membrane increases as the triamterene concentration is increased and this transmembrane potential constitutes the major driving force for Na transport across the luminal membrane. As demonstrated in the section Preliminary Experiments this driving force is not constant. The driving force increases as the Na-sites are blocked. Therefore there will be a tendency to reduce the $1/I_{sc}$ at higher blocker concentrations and to obtain too high values for $K_{b'}(I)$ [see Eq. (5)]. This may be the explanation for the higher mean values for $K_{b'}(I)$ compared with $K_b(f_c)$ as seen in Fig. 7, although the difference is not statistically significant.

The $K_{b'}(I)$ of the Na-concentration is found to be weakly dependent on the Na-concentration, $K_{b'}(I) = (22.6 \pm 0.8) + \text{Na}(0.21 \pm 0.11)$. Independence of the Na-concentration for $K_{b'}(I)$ has probability less than 0.005. The weak dependence of $K_{b'}(I)$ on the Na-concentration means that there is close to noncompetitive kinetics for sodium and triamterene. Thus there seems to be a physical separation of the blocker-site for triamterene from the blocker-site for Na itself.

The consistency of the K_b determined by the two methods is also taken as an indication of the reliability of the current fluctuation analysis, since for noncompetitive kinetics as found for the coprodeum these two K_b 's should be identical.

Noncompetitive kinetics has also been found for the interaction between Na and amiloride in the coprodeum (Cuthbert et al., *in preparation*) as well as for several species of frogs and toads (Benos, Mandel & Balaban, 1979). The only exception is the skin of the European frog (*Rana temporaria*) which has a strong competition between Na and amiloride at the blocking site for the Na-channel (Cuthbert & Shum, 1974; Benos et al., 1979).

Benos, Mandel and Simon (1980) have established evidence for a physical separation of the Na- and the amiloride-blocking-sites in the bullfrog skin which has noncompetitive kinetics. In this frog skin a sulphhydryl-group may be involved at the Na-blocking site and an amino-group at the blocking site for amiloride.

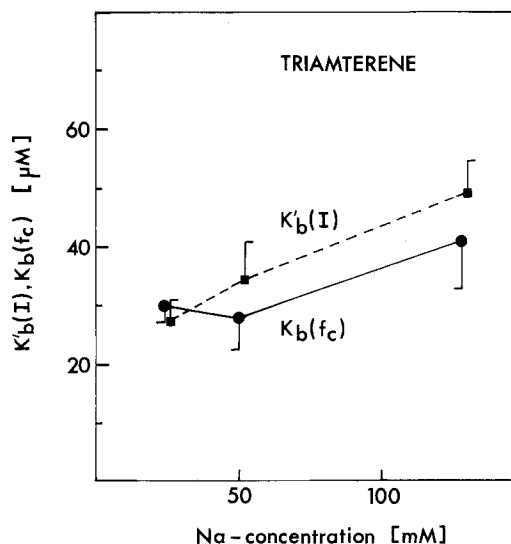


Fig. 7. Variation with sodium concentration of the affinity constant $K_b(f_c)$, derived from analysis of corner frequencies and of the affinity constant $K_{b'}(I)$, derived from analysis of the short-circuit current. $K_b(f_c)$ reflect the site-triamterene interaction whereas $K_{b'}(I)$ reflect the site-sodium-triamterene interaction. The data are mean and SEM based upon 7 to 18 observations

Principal Differences Between $K_{b'}(I)$ and $K_b(f_c)$

The two affinity constants $K_{b'}(I)$ and $K_b(f_c)$ may differ. In the case of two blockers, $1/I_{sc}$ as a function of the blocker concentration will yield an apparent affinity constant. The affinity constant for a blocker determined from I_{sc} is dependent on the rate constants for all the partial processes around equilibrium in the reaction scheme for the interaction of the present blockers with the Na-site. Contrary the current fluctuation-analysis yields in the present case the true affinity constant for triamterene.

When the concentration of Na is altered the determination of the true K_b for triamterene by fluctuation-analysis may nevertheless be affected in various ways of which we shall mention three. Firstly, if the corner frequencies for the two blockers are in the neighborhood of each other there will be an interference with the assessment of the rate constants for triamterene by rate constants for Na. This possibility is ruled out in the present results for the coprodeum, since the corner frequencies for Na-blockade are less than 1 Hz (Christensen & Bindslev, *unpublished*) and the corner frequencies for triamterene are around 50 to 275 Hz. Interference is a possibility in the frog skin study by Van Driessche and Lindemann (1979) because amiloride has corner frequencies much closer to those of Na, about 10 Hz. Secondly, surface characteristics of the epithelium such as the surface charge density could be altered by replacing Na with another cation which in turn might affect the rate constants. Changes in the surface charge seem to interfere with the amil-

oride rate constants in the bullfrog skin (Benos et al., 1980). Thirdly, the rate constants of triamterene could be influenced directly at their blocker-sites by the cation that substitutes for Na, or as a last possibility by a change in the concentration of Na. These three last possibilities could explain the weak dependence of k_2 for triamterene on changes in the Na-concentration, shown in Fig. 7.

High Na Diet Birds

Coprodea from birds on a high Na diet have low I_{sc} around $7 \mu\text{A cm}^{-2}$ (Bindslev, 1979). Triamterene or amiloride does not increase the current fluctuations in the frequency band 2–800 Hz. The background power density spectrum is the same as in the coprodea from hens on a low Na diet and both are significantly reduced by 10^{-4} M ouabain. The background noise is thus most likely due to an ionic gradient, kept by the (Na/K)-ATPase pump, that dissipates through a passive leak. The ionic gradient may therefore consist of a potassium concentration difference.

Very competent design and construction of the electrical set-up was performed by Mr. S. Christoffersen. Machinist K.J. Sørensen assisted during the development of the transport chamber. We appreciate the skilled technical assistance of lab-tech. B. Søndergaard. This work was supported by the NOVO foundation.

References

- Aceves, J., Cuthbert, A.W., Edwardson, M.J. 1979. Estimation of the density of sodium entry sites in frog skin epithelium from the uptake of [^3H] benzamil. *J. Physiol. (London)* **295**:477–490
- Benos, D.J., Mandel, L.J., Balaban, R.S. 1979. On the mechanism of the amiloride-sodium entry site interaction in anuran skin epithelia. *J. Gen. Physiol.* **73**:307–326
- Benos, D.J., Mandel, L.J., Simon, S.A. 1980. Effects of chemical group specific reagents on sodium entry and the amiloride binding site in frog skin: Evidence for separate sites. *J. Membrane Biol.* **56**:149–158
- Bindslev, N. 1979. Sodium transport in the hen lower intestine. Induction of sodium sites in the brush border by a low sodium diet. *J. Physiol. (London)* **288**:449–466
- Chen, Y. 1975. Matrix method for fluctuations and noise in kinetic systems. *Proc. Natl. Acad. Sci. USA* **72**:3807–3811
- Chosniak, I., Munck, B.G., Skadhauge, E. 1977. Sodium chloride transport across the chicken coprodeum. Basic characteristics and dependence on sodium chloride intake. *J. Physiol. (London)* **271**:489–503
- Cuthbert, A.W. 1973. An upper limit to the number of sodium channels in frog skin epithelium. *J. Physiol. (London)* **228**:681–692
- Cuthbert, A.W. 1976. Importance of guanidinium groups for blocking sodium channels in epithelia. *Mol. Pharmacol.* **12**:945–957
- Cuthbert, A.W., Fanelli, G.M., Scriabine, A. 1979. Amiloride and Epithelial Sodium Transport. Urban & Schwarzenberg, Baltimore-Munich
- Cuthbert, A.W., Shum, W.K. 1974. Amiloride and the sodium channel. *Naunyn-Schmiedeberg Arch. Pharmacol.* **281**:261–269
- Czerlinski, G.H. 1966. Chemical Relaxation. Dekker, New York
- Eldrup, E., Møllgård, K., Bindslev, N. 1979. Possible sodium channels in the luminal membrane of the hen lower intestine visualized by freeze fracture. In: Hormonal Control of Epithelial Transport. J. Bourguet, J. Chevalier, M. Parisi, and P. Ripoche, editors. Vol. 85, pp. 253–260. INSERM, Paris
- Eldrup, E., Møllgård, K., Bindslev, N. 1980. Possible epithelial sodium channels visualized by freeze-fracture. *Biochim. Biophys. Acta* **596**:152–157
- Fishman, H.M. 1973. Relaxation spectra of potassium channel noise from squid axon membranes. *Proc. Natl. Acad. Sci. USA* **70**:876–879
- Frömter, B., Gebler, B. 1977. Electrical properties of amphibian urinary bladder epithelia. III. The cell membrane resistances and the effect of amiloride. *Pfluegers Arch.* **371**:99–108
- Helman, S.I., Fisher, R.S. 1977. Microelectrode studies of the active Na transport pathway of frog skin. *J. Gen. Physiol.* **69**:571–604
- Hill, T.L. 1971. Approach of certain systems, including membranes to steady state. *J. Chem. Phys.* **54**:34–35
- Janz, G.J., Ives, D.G. 1968. Silver, silver chloride electrodes. *Ann. N.Y. Acad. Sci.* **148**:210–221
- Koefoed-Johnsen, V., Ussing, H.H. 1958. The nature of the frog skin potential. *Acta Physiol. Scand.* **42**:298–308
- Lindemann, B. 1980. The beginning of fluctuation analysis in epithelial ion transport. *J. Membrane Biol.* **54**:1–11
- Lindemann, B., Van Driessche, W. 1977. Sodium-specific membrane channels of frog skin are pores: Current fluctuations reveal high turnover. *Science* **195**:292–294
- Lindemann, B., Van Driessche, W. 1978. The mechanism of Na uptake through Na-selective channels in the epithelium of frog skin. In: Membrane Transport Processes. J.F. Hoffman, editor. Vol. 1, pp. 155–178. Raven Press, New York
- Lyngdorf-Henriksen, P., Munck, B.G., Skadhauge, E. 1978. Sodium chloride transport across the lower intestine of the chicken. Dependence on sodium chloride concentration and effect of inhibitors. *Pfluegers Arch.* **378**:161–165
- Nagel, W. 1975. Reinvestigation of intracellular PD of frog skin epithelium. *Abstr. 5th Int. Biophys. Congr., Copenhagen*. p. 147
- Schultz, S.G., Frizzell, R.A., Nellans, H.N. 1977. Active sodium transport and the electrophysiology of rabbit colon. *J. Membrane Biol.* **33**:351–384
- Segel, I.H. 1975. Enzyme Kinetics. Ch. 3 and 4. Wiley, New York
- Sudou, K., Hoshi, T. 1977. Mode of action of amiloride in toad urinary bladder. An electrophysiological study of the drug action on sodium permeability of the mucosal border. *J. Membrane Biol.* **32**:115–132
- Van Driessche, W., Gögelein, H. 1978. Potassium channels in the apical membrane of the toad gallbladder. *Nature (London)* **275**:665–667
- Van Driessche, W., Lindemann, B. 1978. Low-noise amplification of voltage and current fluctuations arising in epithelia. *Rev. Sci. Instrum.* **49**:32–37
- Van Driessche, W., Lindemann, B. 1979. Concentration dependence of currents through single sodium-selective pores in frog skin. *Nature (London)* **282**:519–520
- Van Driessche, W., Zeiske, W. 1980. Spontaneous fluctuations of potassium channels in the apical membrane of frog skin. *J. Physiol. (London)* **299**:101–115
- Verveen, A.A., DeFelice, L.J. 1974. Membrane noise. In: Progress in Biophysics and Molecular Biology. J.A.V. Butler and D. Noble, editors. Vol. 28, Ch. 5. Pergamon, Oxford
- Verveen, A.A., Derksen, H.E. 1965. Fluctuations in membrane potential of axons and the problem of coding. *Kybernetik* **2**:152–160

Received 4 February 1981; revised 12 May 1981